ISSN: 0975-3583, 0976-2833 VOL14, ISSUE 07, 2023

FORMULATION, CHARACTERISATION AND PHARMACOKINETICS OF FELODIPINE NANOVESICLES FOR TRANSDERMAL DRUG DELIVERY SYSTEM

Anasuya Patil[1], Dr. Gaurav Jain[2], Sudhir R Iliger[3], Mohit Nagar[4], Dr. Nihar Ranjan Kar[5], Shilpi Mishra[6], Sonali Ravindra Pawar[7], Dr. Meenu Rani[8]*

[1]Associate Professor, Department of Pharmaceutics, KLE College of Pharmacy, II Block Rajajinagar, Bengaluru
[2] Professor, Chameli Devi Institute of Pharmacy, Umarikheda, Khandwa Road, Indore
[3] Professor and Head Department of Pharmaceutics, SET's College of Pharmacy, SR Nagar Dharwad, Karnataka
[4] Assistant Professor, R. V. Northland Institute, Dadri, Gautam Budh Nagar, UP
[5] Assistant Professor, Centurion University of Technology and Management, Odisha, India
[6] Assistant Professor, Shree Krishna College of Pharmacy, Ahamad Nagar, Sitapur, Uttar Pradesh,
[7] Assistant Professor, Sinhgad college of Pharmacy Vadgaon Budruk Pune Maharashtra, India
[8] Assistant Professor, Department of Pharmaceutical Education and Research, Bhagat Phool Singh Mahila Vishwavidyalaya, Bhainswal Kalan, Sonipat, Haryana

Corresponding Author: Dr. Meenu Rani
mnrani75@gmail.com

ABSTRACT

In order to achieve increased felodipine delivery via transdermal delivery, the study investigated the parameters for improving various membrane combinations that incorporate lecithin derived from soy and eggs, in addition to an edge activator. This was done in order to achieve increased transdermal delivery. The Components and the Processes An approach known as rotational evaporation sonication was used in order to bring about the creation of a tranfersomal formulation. All of the following aspects of the formulation were evaluated and analysed: the polydispersity index, also known as the PDI, the zeta potential, the efficacy of trapping and loading, the deformability index, and in vitro skin penetration. Results: It was discovered that the best formulation would consist of spherical nanovesicles with a size of 75.71 5.4 nm, a PDI of 0.228, and a zeta potential of 49.8. (MF8). The fact that MF8's deformability index is so high—119.68—suggests that it attained the maximum degree of loading efficiency and entrapment possible. As compared to the transdermal control formulation, MF8's in vitro permeation through rat skin showed a 256% increase in permeability (flux = 23.72 0.64), with zero-order kinetics. This was in contrast to the transdermal control formulation, which improved permeability.This was determined by comparing the results to the transdermal control formulation (Case-II). Studies on the pharmacokinetics of the drug indicated that when transdermal therapy was compared to oral administration, the transdermal treatment resulted in a generally stable and maintained blood concentration with low plasma change, as well as a rapid and prolonged peak duration. The findings of confocal laser scanning microscopic studies, which showed that the medication quickly penetrated through dermal layers, were compatible with the relative bioavailability of

ISSN: 0975-3583, 0976-2833 VOL14, ISSUE 07, 2023

felodipine, which was found to be 358.42% compared to oral administration. The results demonstrate that felodipine-loaded transfersomes are transcendent because they show that modifying the composition and manufacturing process had a significant influence on the features of the vesicles.

Keywords: Felodipine, Nanovesicles, Transdermal Drug Delivery

INTRODUCTION

Most commonly used to treat hypertension and angina pectoris is felodipine (ethyl methyl 4-(2,3-dichlorophenyl)-1, 4-dihydro-2, 6-dimethyl-3, 5-pyridine dicarboxylate), a calcium channel antagonist. Ethyl methyl 4-(2,3-dichlorophenyl)-1, 4-dihydro-2, 6-dimethyl-3,5 pyridine is its chemical name. [1] Due to substantial hepatic first pass metabolism, it has a bioavailability of 15-20% and is marketed in tablet dose form (2.5–10 mg) for oral administration. It also has the added issue of a dose-dependent deleterious impact that increases proportionately with dosage size. [2] As a result, it became important to explore for other approaches that would make the administration of felodipine less dangerous and more suited to the patient's comfort. Many researchers investigated the issue of eliminating hepatic first-pass metabolism through the transdermal route, and they created both traditional and modified drug delivery techniques. While the transdermal method of drug delivery has clear benefits in terms of being user-friendly and noninvasive, its usage has been limited by the skin's built-in protective barrier qualities, notably the stratum corneum. This is due to the skin's built-in defence mechanism, which functions as a barrier to prevent foreign objects from penetrating the skin. In order to administer felodipine through transdermal administration, solid lipid nanoparticles (SLN) were developed by Ren et al. as a result, the primary focus of felodipine transdermal delivery research has been on discovering various strategies to avoid the issues related to penetration. [3] It has been shown that the transdermal systemic delivery approach is less effective than the localised topical therapeutic use of this technology. [4] In addition, these carriers eject the drug while it is being kept, have a modest drug payload, and form SLN dispersions with a high water content. [5] Transdermal patches containing felodipine and metoprolol were proposed by Wang and colleagues as a maintenance therapy. [6] The newly developed approach demonstrated improved bioavailability but at the cost of a longer lag time. Similar to this, Diez et al. developed a transdermal patch [7] that combined the penetration enhancer with felodipine (d-limonene). The lag time was reduced by this patch from nine hours to one and a half. A lag time of 1.5 hours is excessive and might reduce the effectiveness of the patches' intended use. Moreover, using a permeation enhancer for a lengthy period of time might irritate and harm the skin's immune system. [8] The approach of giving felodipine through transdermal application of deformable lipid vesicles has been put into consideration in an effort to enhance the administration of the medication.

Transfersomes are lipid and edge activator-based vesicular carriers that are self-optimizing, very flexible, and enable better transdermal administration. They are based on edge activators and have inheritable skin-penetrating abilities. Many studies have shown that these materials can penetrate healthy skin and deliver drugs in therapeutic doses when they are used on an open biological barrier in nonocclusive conditions. [9,10] The most crucial element in

ISSN: 0975-3583, 0976-2833 VOL14, ISSUE 07, 2023

improving transfersome penetration across skin is the liquid-state vesicle system with a very flexible lipid bilayer [11]. Because of this arrangement, transfersomes may easily pass through exceedingly small openings when a hydration gradient is present. The vesicle is able to deform without compromising the integrity of its overall structure because it has an edge activator. Edge activators have evolved a variety of stress-dependent adaptations that lessen the barrier to their flow through narrow channels and enable the noninvasive delivery of drugs. This is because they have a tendency to congregate at highly stressed areas and curved structures [12]. The objective of the ongoing study is to use transfersomes to increase felodipine's bioavailability in a safe manner. In order to obtain therapeutic blood levels, this will be done by preventing substantial hepatic first-pass metabolism, keeping a sufficient quantity of the medication on the skin for a long length of time, and administering it systemically[13].

2.MATERIALS AND METHODS

The drug felodipine was provided to us free of charge by AstraZeneca Pharma India Ltd. (Karnataka, India). Himedia Labs Pvt. Ltd. supplied both the egg lecithin and the soya lecithin that were purchased (Mumbai, India). We got our hands on some Tween-80, Span-80, and chloroform from SD Fine-Chem Ltd. (Mumbai, India). New Drug House (P) Ltd. was the vendor for the rhodamine red that was purchased (New Delhi, India). From Qualikems Fine Chemical Pvt. Ltd., we acquired some methanol, ethanol, and isopropyl alcohol (New Delhi. India). Merck Specialty Pvt. Ltd. was the supplier for the Millipore nylon membrane filters that were acquired (Mumbai, India). Other than that, we only utilised analytical-grade reagents for everything else. All experiments on animals have been carried out in full accordance with the ethical and regulatory principles of the institution, as well as in accordance with the spirit of the Association for Assessment and Accreditation of Laboratory Animal Care and in accordance with the international expectations for animal care and use/Ethics Committees. After receiving permission from the Institutional Animal Ethics Committee (IAEC No.: IAEC/RAP/3648a), the studies were carried out. The investigation is broken down into four distinct parts: the preliminary trials, the formulation development, the dosage form design, and the in vivo pharmacokinetic research.

Preliminary Research

Optimization of vortexing and sonication time

The lipid/edge activator ratio was set to 95:5, and felodipine at a concentration of 1% percent w/w was added to the mixture. Entrapment efficiencies were determined after vigorously stirring the mixture for 15, 30, 45, and 60 minutes. The size of the Zetasizer vesicle was important in selecting the ideal sonication time (Malvern Mastersizer, Malvern Co., Worcestershire, UK). The time point that would result in the formation of ideal-sized vesicles with low polydispersity index (PDI) values was chosen.

Drug loading concentration optimisation

The ratio of lipid to edge activator, 95:5, was mixed with felodipine at concentrations of 0.25, 0.50, 0.75, 1.00, 1.25, and 1.50% weight-per-weight, and the effect of these concentrations on entrapment efficiency was analysed (EE). The concentration of felodipine that resulted in the maximum quantity of drug entrapment was selected as the ideal value for this parameter. In

ISSN: 0975-3583, 0976-2833 VOL14, ISSUE 07, 2023

order to determine whether or not there was any drug entrapment, the centrifugation method described in the next section was carried out.

Optimization of the Lipid: Edge activator ratio

Transfersomes were produced by utilising lipids and edge activators at three different levels [Table 1] by using the vortexing sonication method, taking into consideration all of the pre-optimized processing parameters, and being assigned the codes F1-F12 respectively (preliminary formulations). After combining lipid, edge activator, felodipine (1% w/w), and 10 ml of phosphate buffer with a pH of 6.8 in a vortex tube, one should continue to vortex the mixture for a period of thirty minutes. After being sonicated for 30 minutes at 33.3 KHz with an input voltage of 170-250 V AC using a bath sonicator (PCI Analytics, Mumbai, India), the resulting milky solution was extruded through a succession of Millipore nylon membrane filters with 450, 200, and 100 nm pore sizes and stored at 4°C.

Ingredients	**Formulation Code**											
	F1	**F2**	**F3**	**F4**	**F5**	**F6**	**F7**	**F8**	**F9**	**F10**	**F11**	**F12**
Felodipine (mg)	10	10	10	10	10	10	10	10	10	10	10	10
Soya lecithin (%)	95	90	85	-	-	-	95	90	85	-	-	-
Egg lecithin (%)	-	-	-	95	90	85	-	-	-	95	90	85
Tween-80 (%)	5	10	15	5	10	15	-	-	-	-	-	-
Span 80 (%)	-	-	-	-	-		5	10	15	5	10	15

Selected Formulation code	**Modified formulation code**	**Drug (% w/w)**	**Soya lecithin (% w/w)**	**Egg lecithin (% w/w)**	**Tween-80 (% w/w)**	**Span-80 (% w/w)**	**Ethanol: chloroform**
F2	**MF2**	1	90	-	10	-	6:4
F5	**MF5**	1	-	90	10		6:4
F8	**MF8**	1	90	-	-	10	6:4
F11	**MF11**	1	-	90	-	10	6:4

Gel Code	**Drug(mg)**	**Carbopol934P (% w/v)**	**Triethanolamine (% v/v)**	**Ethanol (% v/v)**	**Menthol (% w/w)**	**Double distilled water (ml)**
TG	MF8 Eq. to 10 mg	**1**	**2**	-	-	**10**

ISSN: 0975-3583, 0976-2833 VOL14, ISSUE 07, 2023

	of drug					
CG		**1**	**2**	**1**	**1**	**10**

Characterization of preliminary formulations

Selected Formulation code	Vesicle size (nm)	PDI	Zeta potential	Entrapment efficiency (%)	Loading efficiency (%)
F1	132.4±5.4	0.43	−39.6	71.62±2.42	1.432±0.11
F2	118.4±8.9	0.46	−39.7	79.44±2.3	1.588±0.17
F3	157.8±7.2	0.51	−34.0	73.21±1.97	1.464±0.09
F4	262.2±9.6	0.62	−39.7	69.57±2.95	1.391±0.10
F5	287.3±12.4	1		78.97±1.6	1.578±0.22
F6	222.0±11.2	0.31		70.24±2.21	1.404±0.15
F7	128.4±18.1	0.24	−35.6	72.22±1.24	1.440±0.13
F8	111.5±8.5	0.28	−44.0	80.14±3.1	1.602±0.18
F9	152.9±5.7	0.27	−30.7	70.26±1.90	1.404±0.16
F10	238.7±7.9	0.54	−33.8	69.24±1.21	1.385±0.12
F11	260.8±11.4	0.9	−23.2	73.51±1.89	1.470±0.11
F12	109.2±10.8	0.42	−36.9	70.20±2.31	1.404±0.08

Selected Formulation code	Deformability index	Cumulative drug permeation% (24 h)	Skin deposition (%)	Transdermal flux (Jmax (μg/h/cm^2)
F1	68.97	63.02±1.98	3.38±0.54	16.25±0.34
F2	121.7	75.06±1.89	5.40±0.37	17.63±0.41
F3	139.29	67.28±2.98	3.58±0.72	16.82±0.16
F4	67.26	60.48±1.65	2.98±0.62	15.10±0.27
F5	74.12	67.15±1.75	3.41±0.71	16.77±0.59
F6	95.19	62.56±1.20	3.08±0.97	15.62±0.36
F7	84.27	67.98±1.64	3.40±0.82	16.99±0.21
F8	109.97	78.94±0.99	7.90±0.85	19.73±0.82
F9	129.42	69.42±1.88	3.88±0.74	17.35±0.42
F10	81.37	70.03±1.87	4.32±0.27	17.50±0.33
F11	85.62	72.99±1.22	4.71±0.93	18.49±0.61
F12	102.49	71.52±2.01	3.65±0.28	17.88±0.57

ISSN: 0975-3583, 0976-2833 VOL14, ISSUE 07, 2023

Selected Formulation code	Vesicle size (nm)	PDI	Zeta potential	Entrapment efficiency (%)	Loading efficiency (%)
F2	118.4±8.9 0.458	−39.7	79.44±2.3	1.588±0.17	121.71
MF2	94.71±4.7 0.285	−42.5	84.16±1.72	1.683±0.12	127.59
F5	287.3±9.5 1.00	−39.4	78.97±1.6	1.578±0.22	74.12
MF5	123.3±6.2 0.228	−40.9	83.21±1.24	1.664±0.23	87.54
F8	111.5±5.6 0.277	−44.0	80.14±3.10	1.602±0.18	109.97
MF8	75.71±5.4 0.255	−49.8	85.14±1.39	1.702±0.17	119.68
F11	260.8±7.6 0.902	−23.2	73.51±1.89	1.470±0.11	85.62
MF11	102.3±4.9 0.288	−33.7	78.24±1.92	1.564±0.39	99.86

Selected Formulation code	Deformability index	Cumulative drug permeation% (24 h)	Skin deposition (%)	Transdermal flux (Jmax (µg/h/cm^2)
F2	70.06±2.37	17.63±0.41	5.4	118.4±8.9 0.458
MF2	88.5±1.65	21.63±0.52	6.97	94.71±4.7 0.285
F5	67.15±1.92	16.77±0.59	3.41	287.3±9.5 1.00
MF5	76.82±1.20	19.20±0.36	4.21	123.3±6.2 0.228
F8	78.94±3.76	19.73±0.82	7.9	111.5±5.6 0.277
MF8	94.91±1.88	23.72±0.64	8.15	75.71±5.4 0.255
F11	73.99±3.21	18.49±0.61	4.71	260.8±7.6 0.902
MF11	82.57±1.64	20.64±0.27	4.92	102.3±4.9 0.288

Determination of vesicle size, polydispersity index and zeta potential

ISSN: 0975-3583, 0976-2833 VOL14, ISSUE 07, 2023

The Malvern Master Sizer used laser diffraction-based light scattering to assess the vesicle size, PDI, and zeta potential of the produced transfersomes after appropriately dilution the sample with water as a surfactant.

Deformability studies

The vesicle solution was pushed at 1.2 megapascals (MPa) through a Millipore nylon membrane filter with a pore size of 50 nanometers for ten minutes. A deformability index was constructed to represent the deformability of the material by using the equation that is shown below:

$$\text{Deformability index} = j \times (rv/rp)^2 \quad (1)$$

Where, jis the weight of the suspension, rv the size of the vesicle and rp the pore size of the membrane.

Determination of entrapment efficiency and loading efficiency

Purified transfersomal suspensions were spun at a speed of 10,000 rpm for ten minutes at a temperature of 4 degrees Celsius in a cooling centrifuge (REMI Instrument Ltd., C-24BL/CPR24 Vasai, India) to make pellets that had settled. Before checking for vesicle disruption, the pellet was washed in distilled water to remove any free felodipine, and then it was placed in a test tube containing isopropyl alcohol that had been diluted to a ratio of 50 percent by volume. In addition to that, it was subjected to vortexing, filtration, and spectrophotometric analysis at 237 nm (Shimadzu Corp., Pharmaspec 1700, Kyoto, Japan). For the purpose of calculating the EE and loading efficiency, the following formulas were utilised:

$$\% \text{ EE} = \text{Amount of drug present in vesicles/total drug incorporated} \times 100 \quad (2)$$

$$\% \text{ Loading efficiency} = \text{Amount of drug present in vesicles/total amount of lipid incorporated} \times 100 \quad (3)$$

Ex vivo skin permeation

After being extracted, shaved, and separated, the underlying tissues of the rat skin were examined. The skin that had been removed was placed on a Franz diffusion cell that had an inner dimension of 2.03 cm2 (square centimetres). A preset amount of transfersomal suspension with an identical dose of felodipine was applied to the dorsal side of the skin (donor compartment side). After adding 15 cc of phosphate buffer with a pH of 6.8 and agitating the mixture at 100 rpm, the receptor compartment was heated to 37 degrees Celsius plus 0.5 degrees Celsius. Aliquots of one millilitre were removed from the receptor compartment at the following time intervals: 0 hours, 2 hours, 4 hours, 8 hours, 10 hours, 12 hours, 14 hours, 16 hours, 18 hours, 20 hours, and 24 hours. These aliquots were then replaced with an equivalent quantity of fresh medium. In order to calculate the steady-state flux, a plot of the total amount of felodipine that was absorbed through the skin per unit area over the course of time was performed (Jss),

$$\text{Jss} = \text{Amount of drug permeated/time} \times \text{area of permeation} \quad (4)$$

Skin deposition

The skin that was removed during the in vivo permeation experiment was used to calculate the amount of felodipine that was present inside the skin (after 24 hours). The skin was divided into minute pieces, homogenised by sonication with 95% ethanol by volume, and then left to rest at room temperature for six hours after being rinsed five times with phosphate

ISSN: 0975-3583, 0976-2833 VOL14, ISSUE 07, 2023

buffer pH 6.8 kept at 45 degrees Celsius. The resulting solution was then separated into its supernatant using centrifugation for ten minutes at 8,000 rpm. The supernatant was then examined using a validated high performance liquid chromatography (HPLC) method, which was covered in the following section.

Formulation development:

Alterations were made to the selected preliminary compositions (F2, F5, F8, and F11) by the application of the rotary evaporation sonication method. These compositions included lipid and Edge activator (95:5). After dissolving the lipid, edge activator (95:5), and felodipine (1% w/w) in ethanol and chloroform (3:2), the mixture was then transferred to a 250-ml round-bottom flask that was attached to a rotary vacuum evaporator. This process was repeated until the desired concentration was reached (Macro Scientific Works Pvt. Ltd., New Delhi, India). In order to create a film with a uniformly thin layer, the solution was repeatedly spun while it was being dried in a vacuum. The dried film was rehydrated by constantly whirling it at a rate of 100 revolutions per minute while simultaneously adding 30 millilitres of phosphate buffer to it at a temperature of 45 degrees Celsius. The buffer had a pH of 6.8. After setting the vesicular suspension aside for two hours, sonicating it in a bath using a bath sonicator, and then extruding it, we were able to create transfersomal suspensions, which we designated as MF2, MF5, MF8, and MF11, respectively, in Table 2. The transfersomal suspensions were created by sonicating the vesicular suspension in a bath using a bath sonicator. In order to characterise the formulations with respect to their physical (vesicle size, PDI, zeta potential, entrapment, and loading efficiency) and performance properties, the approaches that were presented before were used (ex vivo permeation studies, flux determination, and skin deposition).

Transmission electron microscopy:

The chosen transfersomal formulation (MF8) was dropped over a copper grid covered in carbon for two minutes, then it was adsorbed using filter paper and negatively stained with phosphotungstic acid. A 300 kV accelerating voltage was used to see the air-dried sample with a transmission electron microscope at 10-100 K magnification (JEOL JEM-3100F, Munchen, Germany).

Differential scanning calorimetry:

Thermal behavior of felodipine and its compatibility with other formulation ingredients was estimated using differential scanning calorimeter (NETZSCH DSC 200F3-240-20-427-L, USA) equipped with an intracooler. The samples were hermetically sealed in aluminum pans and heated at a constant rate of 10°C/min over a temperature range of 0-450°C. An inert atmosphere was maintained by purging with nitrogen at a flow rate of 60 ml/min.

Stability studies:

The chosen formulation (MF8) conducted a three-month stability testing at 4°C and 25°C. Vesicle size and % drug retention were assessed in the samples taken at various time intervals. Any variation seen over time and at various temperatures was noted.

Dosage form design:

Formulation this study used the dispersion technique to create MF8 as a transfersome gel (TG), and it was compared to a control gel (CG). To create its aqueous dispersion, carbopol 934P was immersed in distilled water for two hours at a concentration of 1% weight-per-

ISSN: 0975-3583, 0976-2833 VOL14, ISSUE 07, 2023

volume (w/v). In order to create two distinct compositions, the transfersomal suspension (equivalent to 10 mg) and the pure felodipine solution (also equivalent to 10 mg) were each separately combined in gel bases. Table 1 compares and contrasts these two compositions. The pH of the gel(s) was determined using a digital pH metre (Hanna Instrument Ltd., Italy), and the viscosity of the gel(s) was determined using a Brookfield viscometer R/S-CPS and a T-spindle S-93 at 20 revolutions per minute (22.36 103 g). To determine how much drug was in the sample, a spectrophotometric analysis was carried out. In order to conduct an ex vivo skin permeation investigation using gels, rat skin was placed on top of a Franz diffusion cell. This work's objective was to gauge the steady state flux (Jss). The experiment lasted all day at a temperature of 37 0.5 degrees.

Confocal laser scanning microscopy:

Over the course of the research, Wistar rats served as the subjects, and these animals were divided evenly into control and treatment groups (n = 2/group). The animals went without food but had unrestricted access to water throughout the night. Following that, both the control group and the treatment group had 1 g of CG and a tranfersomal gel containing rhodamine applied to the skin on the dorsal side of the animals' bodies (an area that measured 2 cm2 in total). When the experiment had been going on for a total of six hours, a heart puncture was used to euthanize one animal from each of the treatment and control groups. After that, the dorsal skin was peeled off, well cleaned, and laid out on some aluminium foil. After that, the skin samples were sliced between 10 and 15 millimetres thick (Microtome India, Spencer, New Delhi, India). After waiting for 12 hours, the next two animals were slaughtered and processed in the same manner as described before. Research using confocal laser scanning microscopy (CLSM) was carried out on the skin after it had been cleansed and fixed. The slide was illuminated with a laser with a wavelength of 540 nm, and observation was performed at a magnification of 100 times. After six and twelve hours, respectively, it was feasible to establish the depth that rhodamine-loaded TG and CG had travelled by using the micrographs that were taken.

Pharmacokinetic studies:

Study design:

Wistar rats weighing between 100 and 150 g and having a total of four animals each made up the control group and the test group. The rats were individually given a cage and given permission to fast for the whole night. At any moment, water may be drank at will. The test group mice were given an equivalent amount of TG, whereas the control group animals were given an oral suspension of felodipine (0.15 mg/kg) in 2 ml of water. This was done to guarantee that the dosage for the drug was the same for both groups.

Sample collection, preparation and chromatographiccondition:

At 0, 1, 2, 4, 6, 12, 24 and 48 hours, a 0.5 ml blood sample was extracted from each subject using a 26-Gx11/4-in (0.7 mm 30 mm) 2 ml syringe (Dispo Van, HMD, Faridabad, Haryana, India). The samples were kept in heparin-treated polypropylene plasma tubes with a volume of 5 millilitres each (150 USP units of sodium heparin spray coated, 13 mm 7.5 mm, with a BD hemogaurd closer, BD and Co., NJ, and USA). should further centrifuge the plasma at 12,000 rpm in order to eliminate any cellular debris. The obtained samples were centrifuged for 15 minutes at a speed of 3500 rpm in order to separate the plasma, which was then placed

ISSN: 0975-3583, 0976-2833 VOL14, ISSUE 07, 2023

in microcentrifuge tubes (Sigma Aldrich, USA). The supernatant was collected and stored at 20 degrees Celsius before to being analysed. To calculate the felodipine plasma concentration in the supernatant, a validated HPLC assay technique [14] was applied to an HPLC system (Waters, 2695, USA) equipped with a variable-wavelength UV detector (Aquity T UV Ch A) and set to run at 237 nm. This method was employed. The C18 column (Water, BEH, and C18) was the one that was employed, and its measurements were 150 mm by 4.6 mm. The flow rate of the mobile phase was maintained at 0.8 ml per minute throughout the experiment. The mobile phase consisted of acetonitrile and water at a ratio of 80:20 by volume, and it was degassed in a sonicator for 15 minutes after being filtered through a 0.45-nylon membrane filter.

Sample analysis:

Calibration standards in plasma were created by adding a stock solution of felodipine to 100 L of rat plasma that had been left blank. Stock solutions of felodipine (100 g/mL) and nifedipine (10 g/mL) were prepared in methanol at a concentration of 30% by volume. These solutions served as internal standards. In order to produce the secondary standard solutions, the stock solutions were first diluted with methanol at a volumetric concentration of 30 % (v/v). The operating standard solutions were produced by mixing the secondary solutions with the blank plasma. There were a total of eight calibration standards produced, and their final concentrations were 0, 0, 5, 10, and 20 ng/ml respectively. Before being put through an HPLC analysis, each plasma sample was given 50 litres (L) of a solution containing nifedipine as an internal reference.

Pharmacokinetic analysis:

The plasma concentration versus time profile was used to determine the pharmacokinetic parameters (Cmax, Tmax, area under the curve [AUC0-∞], Ka, Ke, $t_{a1/2}$, and $t_{1/2}$). The relative bioavailability (Fr) of felodipine was determined by comparing the AUC0-∞ from transdermal administration to the AUC0-∞ from oral administration (oral). In order to investigate any potential disparities between the computed parameters, a student's t-test without paired samples was carried outA difference was deemed statistically significant in statistical analysis if it had a P value lower than 0.05.

RESULT AND DISCUSSION:

Optimization of process variables

Optimization of Vortexing and sonication time

During the process of vortexing, high shear forces are applied to the sample, which repeatedly generates cavitations in the lipid lamellae and lowers the size of the vesicles. According to the findings, entrapment efficiencies were as follows: 61.1 ± 1.22, 79.44 ± 1.47, 75.55 ± 1.09 and 75.0 ± 0.98 when the vortexing process was carried out for 15, 30, 45, and 60 minutes, respectively. When the composition was vortexed at a slow velocity and for a longer length of time, the data showed that an increase in EE occurred along with the formation of smaller vesicles. The slow annealing of the vesicles is to blame for this issue. As a result, the vesicle bilayer and the felodipine had more time to interact, which led to an increase in the amount of entrapment. [15] On the other hand, when there was an excessive amount of vortexing, the vesicles were subjected to a high amount of shear stress, which resulted in a large reduction in the vesicle size and created stiff vesicles that were smaller in

ISSN: 0975-3583, 0976-2833 VOL14, ISSUE 07, 2023

size and had a lower EE. According to the findings, it was determined that a time of 30 minutes of vortexing was optimal for the vortexing preparation of transfersomes, with the efficiency enhancement (EE) being at its greatest possible level (79.54% 1.47%) Sonication provides a rearrangement of the initial multilamellar organization into smaller vesicles that necessitates sonication of hydrated vesicles. The transfersomal suspensions were sonicated for 15 and 30 min and results indicated that sonication time of 15 min yielded vesicles of 2184 nm, whereas a sonication time of 30 min downsized the vesicle to 102.3 nm. Thus, a sonication time of 30 min was used.

Optimization of loading drug concentration

On increasing the felodipine concentration from 0.25% to 1.0% w/w there was a significant increase in the drug entrapment ($P < 0.02$), but at concentration beyond 1.0% w/w, considerable decrease in the drug entrapment was documented. The increase in the drug entrapment is ascribed to the lipophilic property of felodipine (log P = 3.86) which enables it to distribute in lipid bilayer and get entrapped in the vesicles, but when the lipid layer becomes saturated with drug, the EE becomes limited.[16] This overloading may damage the vesicular membrane leading to drug leakage and lowering the final drug entrapment, hence a drug concentration of 1.0% w/w was selected. [17]

Optimization of formulation components

Twelve experimental formulations, indicated as F1 through F12 in Table 1, were created using the vortexing sonication technique. The size of the vesicle, the EE, and the deformability index of transfersomes were then investigated as a function of the kind of lipid, the type of edge activator, and the ratio of lipid to edge activator.

Effect on vesicle size Polydispersity index and zeta potential

The size of soya lecithin vesicles ranged from 82.9 ± 5.7 nm to 157.8 ± 7.2 nm while that of egg lecithin vesicles ranged from 109.3 ± 10.8 nm to 287.3 ± 12.4 nm [Table 2]. Comparative results indicate significant differences in the size of transfersomes composed of different lipids ($P < 0.02$). [18,19].We discovered vesicle size variation due on lipid chemical composition and packing behaviour. The edge activator type showed that surfactant composition affects vesicle size [20]. An edge activator with a lower hydrophilic-lipophilic balance produced smaller vesicles (HLB). Hence, span 80 vesicles yielded lesser results than hydrophilic edge activator ones (Tween-80). Edge activator vesicle size and HLB are inversely related because to hydrophobicity decreasing surface energy [22]. PDI values ranged from 0.228 to 0.902, and all formulations were heterogeneous except F7, F8, and F9. PDI values below 0.3 are excellent for dispersion system vesicle size homogeneity. All formulations, save F11, have high physical stability. The dividing line between stable and unstable suspensions is usually +30 or 30 mV. Lipids in formulations caused the net negative charge. The vesicles have a net negative charge since the hydration solution's pH was 6.8 and soy and egg lecithin's isoelectric point is 6.2. Non-ionic felodipine, tween-80, and span-80 do not affect charge formation.

Effect on entrapment and loading efficiency

The entrapment and loading efficiency narrowly ranged between 69.24 ± 1.21 –80.14 ± 3.1 and 1.602 ± 0.18 –1.385 ± 0.12 respectively. Maximum drug entrapment was observed with soya lecithin and span 80 containing formulation having lipid:edge activator in 95:5 ratio

ISSN: 0975-3583, 0976-2833 VOL14, ISSUE 07, 2023

while minimum values were observed with vesicle composed of egg lecithin [Table 2]. The effect can be ascribed to intrinsic entrapment ability of the lipid, nature of the drug and their interaction with the edge activator. Several medical investigations have demonstrated that egg lecithin vesicles have a higher EE than soya ones, which is significant for hydrophilic medicines [23]. The effective equivalent may vary due to felodipine's lipophilicity and edge activator-lipid interactions [24]. It also indicates that egg lecithin transfersomes may have lower EEs because soya lecithin vesicles leak less at a given surfactant concentration. This is because soya lecithin vesicles contain less egg lecithin than egg ones. Drug trapping depends on edge activator type. Span-80 vesicles produced more EE than tween-80 [Table 2]. 4.3 and 16.7 HLB values explain the disparity. Lower HLB values make the edge activator lipophilic. The lipid bilayer will interact with it more easily, producing vesicles and increasing medicine entrapment. The lipid to edge activator ratio change showed EE's considerable alterations. High-lipid formulations with low edge activator (98:2) had low effective expendable energy. Nevertheless, boosting edge activator (95:5) significantly increased EE (P 0.002). Edge activator concentration increased to 10% w/w lowered EE [Table 2] [25]. Low concentrations of surfactant monomers are initially incorporated into the lipid bilayer via the partition equilibrium between the aqueous and lipid phases. The vesicle expands slower, trapping less medicine. Vesicles and membrane bilayer fluidity increased with surfactant concentration, raising EE. Increased edge activator concentration solubilizes phospholipids from mixed micelles [26]. These combined micelles generate holes [27] in surfactant-saturated vesicles. Mixed micelles are stiff and low-energy (EE). High edge activator concentrations generate holes, which release vesicles. Drug entrapment decreases and drug loss increases.

Effect on deformability index

The membrane deformability is a result of combination of at least two different amphiphiles (lipid + edge activator) that have totally different packing characteristics into a single bilayer. The deformability index of preliminary formulations ranged widely between 67.26 and 139.29. The deformability index of soya lecithin vesicles was found to be higher than that of egg lecithin vesicles. This is due to the fact that soya lecithin interacts more easily with surfactants and edge activators than egg lecithin does. It is a well-established fact that the incorporation of an edge activator into a membrane bilayer in the form of an intercalator confers flexibility and the ability to generate edges on transfersomes, hence enabling the latter to be deformed. The phenomena on the other hand is, only realistically relevant up to a certain concentration of surfactant. At that concentration, mixed micelles, which are rigid vesicles with very little to no deformability, arise. The results, which are shown in Table 2, demonstrate that the kind of edge activator also had an effect on deformability. Tween-80 included a larger quantity of it as compared to Span-80, which contained vesicles. This might be because of the hydrophilic feature of Tween-80, which led to the formation of transient hydrophilic pores and increased the fluidity-causing amphiphilic property of the membrane bilayer. One such aspect that plays a role in determining deformability is the chemical composition of the edge activator. As shown by span 80, edge activators that have a significant proportion of bulky carbon chain replacement have less capacity to deform. As was shown with Tween-80, the fluidity of the membrane bilayer is increased by replacing rigid carbon chains with flexible and non-bulky ones [28]. There was a discernible pattern in

ISSN: 0975-3583, 0976-2833 VOL14, ISSUE 07, 2023

the link that existed between deformability and the concentration of lipid-edge activator. The vesicles were less able to be deformed at a ratio of 98:2 than they were at a ratio of 95:5, and this decrease in deformability increased even more as the edge activator concentration (90:10) increased. The EE, on the other hand, dropped on a consistent basis, which may have been caused by the formation of vesicle pores or the generation of mixed micelles.

***Ex vivo* skin permeation**

The amount of felodipine permeated though rat skin [Figure 1a] from F1-F12 was found in the range of 60.48 ± 1.65 (F4) to 78.94 ± 0.99 (F8) in 24 h. The experimental flux of all the formulations was compared with the theoretical target flux (24.28 μg/cm^2 /h) to screen out formulations that were considerably closer to the target flux. The flux value [Table 2] varied with the minimum value of 15.10 ± 0.27 μg/cm^2 /h tothe highest value of 19.73 ± 0.82 μg/cm^2 /h correlatable to the formulation F4 and F8 respectively. The findings also demonstrated that felodipine penetration rates were lower for egg lecithin vesicles in comparison to soya lecithin vesicles, which satisfied prior hypotheses regarding vesicle size, drug entrapment, and relative deformability that were not ideal for egg lecithin vesicles. There was a wide range in the percentage of skin deposition, from 2.98 to 7.90. The drug's deposition in the skin was very variable as a result of the fact that transfersomes physical properties, such as vesicle size and deformability, differed significantly from one another. It is possible that the ability of transfersomes to permeate the skin even in non-occlusive conditions and their interaction with the lipid are responsible for the maximum quantity of medicine that was deposited in the skin for F8, which was 7.90% 0.85%. The adjustment in the lipid:edge activator ratio also shown that there is the potential for an influence on the medication release rates. When the edge activator concentration was at its bare minimum, the transdermal flux was at its bare minimum as well (98:2). At 5% w/w (95:5), the maximum transdermal flow was observed, and at 10% w/w (90:10), the flux decreased possibly as a result of the formation of mixed micelles with low EE and no deformability or possibly as a result of pore formation that causes more drugs to leak out of the vesicles. The maximum transdermal flow was observed at 5% w/w (95:5). The pattern was seen in every formulation, notwithstanding the kind and characteristics of the lipid or edge activator; however, the degree of penetration varied depending on these parameters. Mixed micellar systems have lower permeation resistance than other types of systems, but they are unable to elicit a greater flux. This prevents them from opening the tight junctions between the cells and passing through the stratum corneum. This is because mixed micellar systems are unable to react to the transepidermal hydration gradient. [29] The characterization of preliminary formulations showed that transfersomal formulations containing lipid and edge activator in the ratio of 95:5 have preferable properties in terms of physical and performance characteristics when compared to other ratios of 98:2 and 90:10, regardless of the type of lipid or edge activator that was used. Nevertheless, when measured against the target flow, the total drug permeation, permeability coefficient, and flux value of vesicles constructed with a 95:5 ratio came in significantly below expectations. It is possible that the huge vesicle sizes and high PDI values are the result of the vortex sonication process, which results in an improper hydration of the lipid. This method was chosen for screening due to its relatively cheap cost, its feasibility, and the speed with which it produced findings. The formulations that were

ISSN: 0975-3583, 0976-2833 VOL14, ISSUE 07, 2023

made with 95:5 ratios were changed via the use of a different technology in order to improve the product and bring the vesicle size down.

Formulation development

The selected formulations (F2, F5, F8 and F11) were modified by preparing them by rotary evaporation sonication method and coded as MF2, MF5, MF8 and MF11 respectively, characterized and compared with original formulations. These formulations showed significant ($P < 0.002$) improvement in the vesicle size ($75 \pm 3.7 – 123.3 \pm 4.2$ nm) and PDI (0.228-0.285), while insignificant increase in zeta potential was observed in comparison to original formulations [Table 3]. The improvisation in the vesicle size is a result of proper hydration of the thin lipid film formed by rotary evaporation of the solvent resulting in large surface area exposed for hydration that conferred easy hydration of the lipid film and homogenization of vesicles. The zeta potential changed insignificantly ($P > 0.002$) as it depends on the formulation composition that remained unaltered. Similarly, marked improvement in both entrapment and loading efficiencies was recorded in comparison to the original formulation. This was the result of cumulation of numerous factors like increased contact points due to large surface area of the lipid film and slow annealing of vesicles for larger duration. Deformability index that depends on the proper intercalation of edge activators within the lipid improved on the method manipulation.On similar lines, ex vivo permeation studies indicated significant improvement ($P < 0.002$) in the felodipine permeation and the transdermal flux of the modified formulations [Figure 1b]. Among the modified formulations, maximum permeation was achieved by formulation MF8 (94.91%) with a transdermal flux of 23.72 μg/cm2 /h, while the minimum permeation was recorded for MF5 (76.82%, flux = 19.22 μg/cm2 /h). A higher effective energy (EE), lower deformability index, and smaller vesicles increased penetration and flow. They include: As proven with the MF8, successful trapping permits the vesicle to deliver more medicine through the skin, while its smaller size improves skin absorption. The different edge activators in MF8 and MF2 caused the variance in deformability. These discrepancies were covered before. MF8's flux compensated for its lower deformability index. DSC tests of its thermal behaviour and vesicle shape validated it as the optimum formulation.

Vesicle shape

MF8's transmission electron microscopy [Figure 2] shows spherical and little oval vesicles. The structural appearance showed a denser contour encasing a lighter core. When exposed to water, a thin lipid coating forms an enclosed vesicular structure that might be spherical or oval. This arrangement reduces system free energy to enhance thermodynamic stability.

Differential scanning Calorimetry

Differential scanning calorimetry of pure felodipine exhibited a sharp melting endothermic peak at 148.2°C [Figure 3a] that was ascribed to drug melting. DSC of pure soya lecithin exhibited endothermic peaks at 43.2°C, 104.1°C and 205.9°C. In the thermogram, the state below the advent of first endothermic peak at 43.2°C of soya lecithin defines more ordered lamellar gel phase in which the acyl chains remain closely packed and in trans configuration [30]. The peak observed at 43.2°C [Figure 3b] indicated the transition temperature (Tm) at which the gel phase got converted to liquid crystalline state and above this temperature (Tm) trans/gauche rotational isomerism takes place along the acyl chain that expands laterally. As a

ISSN: 0975-3583, 0976-2833 VOL14, ISSUE 07, 2023

result, the thickness and density of bilayer decreases and lipid becomes more fluid.[31] Transition temperature (Tm) is important, while developing vesicles as above Tm, vesicle formation is easy so in the present research hydration temperature of 45°C was selected to obtain liquid crystalline vesicles. The peak observed at 209.5°C may be attributed to the isotropic liquid phase of the lipid. Because of this, an exothermic peak that occurs at 251 degrees Celsius is presumably connected with the release of the bound water, which is an irreversible process after the sample has been heated. This is due to the fact that the thermal analysis was made more difficult than it should have been due to the existence of bound water in the soy lecithin, which could not be entirely removed under normal storage circumstances. This might also explain certain disruptions in the thermogram. [32] As the water is discharged, there is a possibility that crystallisation will occur since the peak is exothermic. Because of the short melting span, the thermogram of lecithin + span 80 exhibited a little decrease in Tm (40.80 degrees Celsius) as well as a broadening of the peak [Figure 3c]. Tm was greatly influenced as a result of the enhanced affinity that Span had for the lipid as a result of its lipophilicity. After physically combining felodipine, soy lecithin, and edge activator, the DSC thermogram of this combination [Figure 3d] showed a single broad peak at 119.4 degrees Celsius. This peak indicates that all of the elements were mixed together in a manner that was consistent throughout the mixture. It is important to notice that MF8 had the same chemical peak [Figure 3e], which indicates that the drug was diluted and solubilized in the molten lipid due to the greater temperature.

Stability

After 90 days, drug loss at 4°C was 0.071 per day, at 25°C, 0.154 per day, and 85.23% of drug was kept. The vesicle transitioning from gel to liquid may induce medication leakage at higher temperatures. As vesicles retain their gel state and packing characteristics at lower temperatures, less medication is lost. When temperature rose, gel-like vesicles became liquid-crystalline. The membrane packing relaxed, making vesicles more flexible and permeable. Storage duration and vesicle size were studied. After 90 days, vesicle size increased from 75.71 to 155.2 nm. This may be caused by the aggregation and fusing of numerous tiny vesicles, which expanded their size. [34] A basic aggregation model predicts that a single vesicle will flocculate and grow. Nevertheless, vesicles may be gently sheared back to their vesicular condition after flocculation. Later fusion and coagulation increase vesicle size irreversibly. [35] MF8 behaved similarly when suspended for longer (ninety days). A gelling substance may inhibit vesicle formation by turning transferosomal fluid into a gel. Transferrin gel production began.

Dosage form design

In order to be effective, a transdermal dosage form has to fulfil a number of stringent requirements, including those pertaining to practicability, stability, sensitivity, therapeutic elegance, and patient compliance. MF8 was formulated into a gel, which was given the designation of [TFG], and then it was evaluated in comparison to a control transdermal gel with regard to numerous criteria, such as pH, viscosity, drug content, and ex vivo drug absorption (CG).

pH, Viscosity and Drug content

ISSN: 0975-3583, 0976-2833 VOL14, ISSUE 07, 2023

Physical examination of gels revealed them as transparent products with a faint smell of raw materials used. The pH of TFG and CG was 6.9 ± 0.16 and 6.8 ± 0.21 respectivelythat was within the specified range of physiological skin pH of 3-9, and rendered the formulations safe and non-irritating to the skin. Viscosity of TFG and CG was found to be 37584.2 ± 7.23 cpand 35945.3 ± 5.97cp that will facilitate the retention of gel on the skin as well as provide easy extrusion of the dosage form from the package. Carbopol 934P was present in both the gels in the same strength, and equal volume has been maintained, still the viscosity of TFG was found to be slightly higher than the CG. This may be attributed to the presence of lipid vesicles in TFG that increased viscosity of the gel. Drug content of TFG and CG was determined and found to be 97.12 ± 1.76 and 98.57 ± 1.91% indicating homogenous dispersion of drug in the gel matrix.

Ex vivo skin permeation

The maximal permeation from TFG was 2.6 times higher (93.91 ± 1.88%) as compared to CG (35.97 ± 1.31%) at 24 h [Figure 1c]. The transdermal flux achieved by the CG was 2.7 times lower (8.90 ± 0.09 μg/cm2 /h) than the target flux (24.28 μg/cm2 /h) and 2.6 times lower than TFG (23.40 ± 0.19 μg/cm2 /h). The drug's poor water solubility may have hindered CG penetration. Despite penetration enhancers and a hydrophilic environment, the medication failed to create a sufficient concentration gradient to penetrate over the skin. Ultra-flexibility and improved drug linkage within lipid bilayers facilitated TFG drug penetration by quickly permeating intact vesicles and partitioning them into the stratum corneum. Both increased TFG drug penetration. [36] Analyzing the gels' drug release kinetics required several kinetic equations. TFG had a correlation of 0.999 and CG 0.975, following the zero order kinetics concepts. The diffusion exponent, or n, of 1.125 and 1.272 showed the Case-II transport mechanism released the drug [37].

Confocal laser scanning microscopy

The dermatomed rat skin was utilised in the study so that the researchers could illustrate how something may potentially penetrate the skin and also analyse the amount of penetration. The stratum corneum thickness in rats is 18 μm, which is similar to the thickness of the stratum corneum in humans (17–20 μm). [38] CLS micrographs (Figure 4) revealed that the fluorescence in the stratum corneum area was substantially lower than that of the CG after a 6-hour TFG treatment. It is probable that this is owing to the transfersomes' extraordinary flexibility, which enabled them to more readily penetrate the stratum corneum while retaining their integrity. [39] Yet, the existence of a weak fluorescence in this location, caused by the interaction of the lipids in the stratum corneum with the vesicles, demonstrates the role of the lipid system in improving penetration.[40-54] A greater fluorescence intensity with CG, on the other hand, revealed that the tracer was predominantly limited to the stratum corneum. Although TFG fluoresced more intensely than CG in the viable epidermal zone, both TFG and CG increased the depth of tracer penetration. TFG, on the other hand, enhanced the depth of tracer penetration more rapidly. As comparison to TFG, CG's fluorescence intensity remained comparatively high all the way down to 109.6 μm, but TFG's intensity began to decline at 38.09 μm. Rhodamine was found in significant concentrations in CLSM micrographs collected 12 hours after the TFG treatment, all the way down to a depth of 142.5 metres. After this, the fluorescence intensity reduced, but it was still detectable at a distance

ISSN: 0975-3583, 0976-2833 VOL14, ISSUE 07, 2023

of 165.6 µm, showing that the tracer infiltrated the upper dermis through the vesicular system. In contrast to TFG, CG remained limited to the epidermis's topmost layer, and fluorescence evidence was difficult to detect down to a maximum depth of 49.2 µm. Based on our data, it seems that TFG-mediated deep and fast permeation behaviour may enhance felodipine pharmacokinetics.

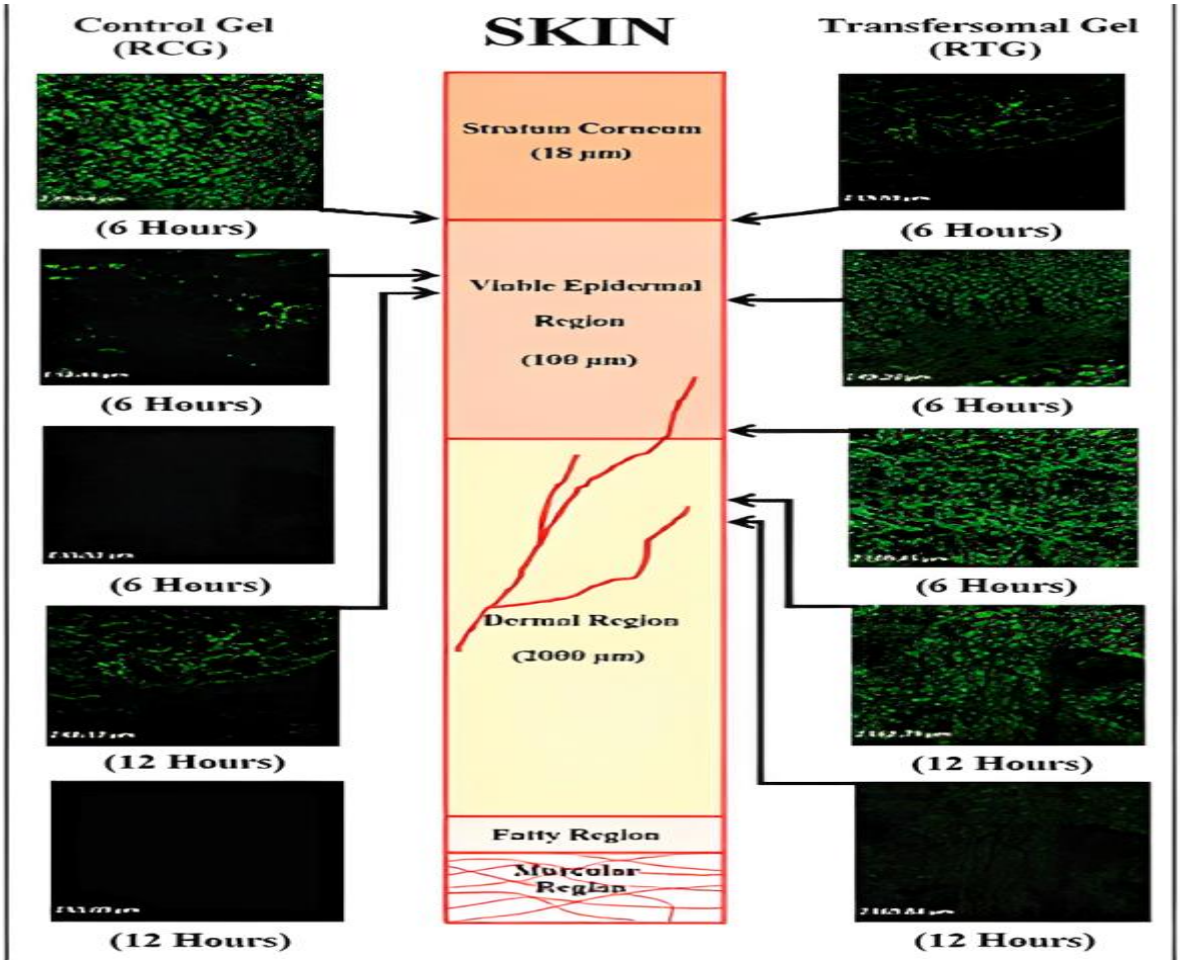

Figure 4: Confocal laser scanning micrographs showing the extent of permeation of rhodamine loaded control gel and rhodamine loaded transfersomal gel, after 6 and 12 h of application

Pharmacokinetics

The plasma concentration-time profile [Figure 5] showed that TFG exhibited higher plasma drug concentration at all-time points than CG. The rapid appearance of drug in plasma is attributed to the high permeation ability of TG when applied under nonoccluded conditions. The peak plasma concentration (Cmax) displayed by TFG was 8.05 ± 0.42 ng/ml while control oral formulation attained 2.31 ± 0.47 ng/ml in 6.0 ± 1.9 and 4.85 ± 2.3 h (tmax) respectively. Considering the data beyond the Cmax, followed first order kinetics, the elimination rate (Ke), was insignificantly different ($P > 0.05$) for TFG and oral control formulation (0.043 ± 0.03 and 0.0602 ± 0.02 h−1 respectively). The absorption rate constant (Ka) was 0.391 ± 0.04 for TFG and 0.267 ± 0.02−h for oral control formulation. The reason for TFG's higher absorption rate was the fast penetration ability of the ultradeformable

ISSN: 0975-3583, 0976-2833 VOL14, ISSUE 07, 2023

vesicular system, which quickly rendered felodipine accessible for absorption. According to the results of the AUC calculation, an improvement in bioavailability is projected to follow from a combination of a greater absorption and a shorter tmax. AUC0-∞ that directly reflects bioavailability was 45.27±6.34 ng.h/ml and 162.26 ± 4.97 ng.h/ml for oral control formulation and TFG. As a result, TFG has a relative bioavailability (Fr) of 358.54%. The increased bioavailability verifies the ex vivo permeation trials, which showed quick drug penetration with low lag time and might be attributable to the avoidance of felodipine's hepatic first-pass metabolism.

CONCLUSION

The outcomes of the present analysis established transfersomes as highly effective transdermal carrier for passive transport of lipophilic and practically water insoluble felodipine. The research also demonstrates the effects of type of lipid and edge activators on the physical and performance characteristic of transfersomes. The combination of soya lecithin and span provided most optimal results and carried maximal drug across the skin. The results of in vivo pharmacokinetic studies and confocal laser scanning microscopic studies depicted rapid permeation of felodipine loaded transfersome to achieve high drug plasma levels with enhanced bioavailability. The research concludes that transfersomes rapidly and noninvasively permeated across the skin to obtain rapid therapeutic drug levels in plasma at lower dose and successfully avoided the hepatic first pass metabolism of felodipine.

REFERENCES

1. Gillmans AG, Hardman JG, Limbird LE. Goodman and Gillman's; The Pharmacological Basis of Therapeutics. 11th ed. New York: McGraw Hill; 2006. p. 296.
2. Murray L, Kelly GL. Physician Desk Reference. 60th ed. Florence: Thomas Healthcare; 2006. p. 221.
3. Ren H, Chang H, Zhang M, Wang W. Study on preparation and skin permeation of solid lipid nanoparticles containing felodipine. J Pharm Pract 2008;5:24-31.
4. Müller RH, Petersen RD, Hommoss A, Pardeike J. Nanostructured lipid carriers (NLC) in cosmetic dermal products. Adv Drug Deliv Rev 2007;59:522-30.
5. Mehnert W, Mäder K. Solid lipid nanoparticles: Production, characterization and applications. Adv Drug Deliv Rev 2001;47:165-96.
6. Wang WG, Yun LH, Wang R, Fu GY, Liu ZY. Preparation of transdermal drug delivery system of felodipine-metoprolol and its bioavailability in rabbits. Yao Xue Xue Bao 2007;42:1206-14.
7. Diez I, Peraire C, Obach R, Domenech J. Influence of d-limonene on the transdermal penetration of felodipine. Eur J Drug Metab Pharmacokinet 1998;23:7-12.
8. Fox LT, Gerber MM, Plessis JD, Hamman JH. Transdermal drug delivery enhancement by compounds of natural origin. Molecules 2011;16:10507-40.
9. Cevc G, Blume G, Schtzlein A, Gebauer D. The skin: A pathway for systemic treatment with patches and lipid-based agent carriers. Adv Drug Deliv Rev 1996;18:349-78.
10. Cevc G, Blume G. New, highly efficient formulation of diclofenac for the topical,

ISSN: 0975-3583, 0976-2833 VOL14, ISSUE 07, 2023

transdermal administration in ultradeformable drug carriers, Transfersomes. Biochim Biophys Acta 2001;1514:191-205.

11. Cevc G, Gebauer D. Hydration-driven transport of deformable lipid vesicles through fine pores and the skin barrier. Biophys J 2003;84:1010-24.
12. El Maghraby GM, Barry BW, Williams AC. Liposomes and skin: From drug delivery to model membranes. Eur J Pharm Sci 2008;34:203-22.
13. Cevc G, Blume G. Biological activity and characteristics of triamcinolone-acetonide formulated with the self-regulating drug carriers, Transfersomes. Biochim Biophys Acta 2003;1614:156-64.
14. Migliorança LH, Barrientos-Astigarraga RE, Schug BS, Blume HH, Pereira AS, De Nucci G. Felodipine quantification in human plasma by high-performance liquid chromatography coupled to tandem mass spectrometry. J Chromatogr B Analyt Technol Biomed Life Sci 2005;814:217-23.
15. Fresta M, Villari A, Puglisi G, Cavallaro G. 5-Flourouracil: Various kinds of loaded liposomes: Encapsulation efficiency, storage stability and fusogenic properties. Int J Pharm 1993;99:145-56.
16. Ning MY, Guo YZ, Pan HZ, Yu HM, Gu ZW. Preparation and evaluation of proliposomes containing clotrimazole. Chem Pharm Bull (Tokyo) 2005;53:620-4.
17. Zucker D, Marcus D, Barenholz Y, Goldblum A. Liposome drugs' loading efficiency: A working model based on loading conditions and drug's physicochemical properties. J Control Release 2009;139:73-80.
18. El Maghraby GM, Williams AC, Barry BW. Oestradiol skin delivery from ultradeformable liposomes: Refinement of surfactant concentration. Int J Pharm 2000;196:63-74.
19. Jain S, Jain P, Umamaheshwari RB, Jain NK. Transfersomes — a novel vesicular carrier for enhanced transdermal delivery: Development, characterization, and performance evaluation. Drug Dev Ind Pharm 2003;29:1013-26.
20. Duangit S, Opanasopit P, Rojanarata T, Ngawhirunpat T. Characterization and *in vitro* Skin Permeation of meloxicam loaded liposomes versus transfersomes. J Drug Deliv. 2011;2011:418316.
21. Yoshioka T, Stemberg B, Florence AT. Preparation and properties of vesicles (niosomes) of sorbitan monoesters (Span 20, 40, 60 and 80) and a sorbitantriester (Span 85).Int J Pharm 1994;105:1-6.
22. El Zaafarany GM, Awad GA, Holayel SM, Mortada ND. Role of edge activators and surface charge in developing ultradeformable vesicles with enhanced skin delivery. Int J Pharm 2010;397:164-72.
23. Nii T, Ishii F. Encapsulation efficiency of water-soluble and insoluble drugs in liposomes prepared by the microencapsulation vesicle method. Int J Pharm 2005;298:198-205.
24. Memoli A, Annesini MC, Petralito S. Surfactant-induced leakage from liposomes: A comparison among different lecithin vesicles. Int J Pharm 1999;184:227-35.

ISSN: 0975-3583, 0976-2833 VOL14, ISSUE 07, 2023

25. Ahad A, Aqil M, Kohli K, Sultana Y, Mujeeb M, Ali A. Formulation and optimization of nanotransfersomes using experimental design technique for accentuated transdermal delivery of valsartan. Nanomedicine 2012;8:237-49.
26. Elorza MA, Elorza B, Chantres JR. Stability of liposomal formulations: Actions of amphiphilic molecules. Int J Pharm 1997;158:173.
27. Edwards K, Almgren, M. Kinetics of surfactant-induced leakage and growth of unilamellar vesicles. Prog Colloid Polym Sci 1990;82:190-7.
28. Rowe RC, Sheskey JP, Owen SC. Handbook of Pharmaceutical Excipients. London: Pharmaceutical Press; 2006.
29. Paul A, Cevc G, Bachhawat BK. Transdermal immunisation with an integral membrane component, gap junction protein, by means of ultradeformable drug carriers, transfersomes. Vaccine 1998;16:188-95.
30. El Maghraby GM, Williams AC, Barry BW. Skin delivery of oestradiol from lipid vesicles: Importance of liposome structure. Int J Pharm 2000;204:159-69.
31. Rolland A, Brzokewciz A, Shroot B, Jamoulle JC. Effect of penetration enhancers on the phase transition of multilamellar liposomes of dipalmitoylphosphatidylcholine: A study by differential scanning calorimetry. Int J Pharm 1991;76:217-24.
32. Fang JY, Hong CT, Chiu WT, Wang YY. Effect of liposomes and niosomes on skin permeation of enoxacin. Int J Pharm 2001;219:61-72.
33. Fang JY, Fang CL, Liu CH, Su YH. Lipid nanoparticles as vehicles for topical psoralen delivery: Solid lipid nanoparticles (SLN) versus nanostructured lipid carriers (NLC). Eur J Pharm Biopharm 2008;70:633-40.
34. Lee EH, Kim A, Oh YK, Kim CK. Effect of edge activators on the formation and transfection efficiency of ultradeformable liposomes. Biomaterials 2005;26:205-10.
35. Sinico C, Manconi M, Peppi M, Lai F, Valenti D, Fadda AM. Liposomes as carriers for dermal delivery of tretinoin: *In vitro* evaluation of drug permeation and vesicle-skin interaction. J Control Release 2005;103:123-36.
36. Simões SI, Delgado TC, Lopes RM, Jesus S, Ferreira AA, Morais JA, *et al.* Developments in the rat adjuvant arthritis model and its use in therapeutic evaluation of novel non- invasive treatment by SOD in Transfersomes. J Control Release 2005 21;103:419-34.
37. Roberts MS, Lai PM, Cross SE, Yoshida NH. Mechanism of Transdermal Drug Delivery. New York: Mercel Dekker; 1997. p. 241-9.
38. Godin B, Touitou E. Transdermal skin delivery: Predictions for humans from *in vivo, ex vivo* and animal models. Adv Drug Deliv Rev 2007;59:1152-61.
39. Bouwstra JA, Honeywell-Nguyen PL. Skin structure and mode of action of vesicles. Adv Drug Deliv Rev 2002;54 Suppl 1:S41-55.
40. Honeywell-Nguyen PL, Bouwstra JA. Vesicles as a tool for transdermal and dermal delivery. Drug Discov Today 2005;2:67-74.

ISSN: 0975-3583, 0976-2833 VOL14, ISSUE 07, 2023

41. Pal N, Mandal S, Shiva K, Kumar B. Pharmacognostical, Phytochemical and Pharmacological Evaluation of Mallotus philippensis. Journal of Drug Delivery and Therapeutics. 2022 Sep 20;12(5):175-81.
42. Singh A, Mandal S. Ajwain (Trachyspermum ammi Linn): A review on Tremendous Herbal Plant with Various Pharmacological Activity. International Journal of Recent Advances in Multidisciplinary Topics. 2021 Jun 9;2(6):36-8.
43. Mandal S, Jaiswal V, Sagar MK, Kumar S. Formulation and evaluation of carica papaya nanoemulsion for treatment of dengue and thrombocytopenia. Plant Arch. 2021;21:1345-54.
44. Mandal S, Shiva K, Kumar KP, Goel S, Patel RK, Sharma S, Chaudhary R, Bhati A, Pal N, Dixit AK. Ocular drug delivery system (ODDS): Exploration the challenges and approaches to improve ODDS. Journal of Pharmaceutical and Biological Sciences. 2021 Jul 1;9(2):88-94.
45. Shiva K, Mandal S, Kumar S. Formulation and evaluation of topical antifungal gel of fluconazole using aloe vera gel. Int J Sci Res Develop. 2021;1:187-93.
46. Ali S, Farooqui NA, Ahmad S, Salman M, Mandal S. Catharanthus roseus (sadabahar): a brief study on medicinal plant having different pharmacological activities. Plant Archives. 2021;21(2):556-9.
47. Mandal S, Jaiswal DV, Shiva K. A review on marketed Carica papaya leaf extract (CPLE) supplements for the treatment of dengue fever with thrombocytopenia and its drawback. International Journal of Pharmaceutical Research. 2020 Jul;12(3).
48. Mandal S, Vishvakarma P, Verma M, Alam MS, Agrawal A, Mishra A. Solanum Nigrum Linn: An Analysis Of The Medicinal Properties Of The Plant. Journal of Pharmaceutical Negative Results. 2023 Jan 1:1595-600.
49. Vishvakarma P, Mandal S, Pandey J, Bhatt AK, Banerjee VB, Gupta JK. An Analysis Of The Most Recent Trends In Flavoring Herbal Medicines In Today's Market. Journal of Pharmaceutical Negative Results. 2022 Dec 31:9189-98.
50. Mandal S, Vishvakarma P, Mandal S. Future Aspects And Applications Of Nanoemulgel Formulation For Topical Lipophilic Drug Delivery. European Journal of Molecular & Clinical Medicine.;10(01):2023.
51. Chawla A, Mandal S, Vishvakarma P, Nile NP, Lokhande VN, Kakad VK, Chawla A. Ultra-Performance Liquid Chromatography (Uplc).
52. Mandal S, Raju D, Namdeo P, Patel A, Bhatt AK, Gupta JK, Haneef M, Vishvakarma P, Sharma UK. Development, characterization, and evaluation of rosa alba l extract-loaded phytosomes.
53. Mandal S, Goel S, Saxena M, Gupta P, Kumari J, Kumar P, Kumar M, Kumar R, Shiva K. Screening of catharanthus roseus stem extract for anti-ulcer potential in wistar rat.
54. Shiva K, Kaushik A, Irshad M, Sharma G, Mandal S. Evaluation and preparation: herbal gel containing thuja occidentalis and curcuma longa extracts.